https://doi.org/10.48047/AFJBS.6.12.2024.4472-4481

African Journal of Biological Sciences

Journal homepage: http://www.afjbs.com

Research Paper Open Access

The development of two-dimensional perovskite solar cells that are more stable and efficient.

Mrs.Padmashri Sujit Dharmpatre
Researcher at Swami Vivekanand University Sagar,Madya Pradesh

Dr.Sandhya Patel
Professor at Swami Vivekanand University Sagar,Madya Pradesh

Article History
Volume 6, Issue 12, 2024
Received: June 10, 2024
Accepted: July 5, 2024
doi:
10.48047/AFJBS.6.12.2024.4472-4481

ABSTRACT:
Pervskite sun-powered cells certainly stand out from scientists overall because of their fast turn of events and proficiency. In any case, strength is as yet an issue that restricts the development of this innovation. The fabrication and characterization of two-dimensional perovskites of the are presented in this work. Ruddlesden-Popper's family (A)2(MA)n−1PbnI3n+1 (three unique A-site huge cations were researched: A=n-propylammonium, t-Butylammonium or Benzylammonium). The materials' band gap got wider as a result of the modulation of the large organic cations. and improved thermal and moisture resistance, making it possible to manufacture PSCs. The remarkable efficiency of 10.35 percent and superior stability of (BUA)2(MA)2Pb3I10 made it possible to retain 68% of its initial value after 1700 h for devices without encapsulation, despite the fact that the organic interlayers intrinsically reduce the transport properties of the devices and, as a result, lower currents are obtained in the layered systems.

RESUMEN:
Due to significant advancements in their efficacy, Perovskite solar cells have attracted scientific attention in recent years. Sin ban, su estabilidad es todavía un problema que limita el avance de esta tecnología. The fabrication and characteristics of bisexual pervoskitas belonging to the Ruddlesden-Poppery family (A)2(MA)n1PbnI3n+1 are presented in this study (three major cations were studied in position A: n-propilamonio, t-Butilamonio, or Bencilamonio). The modulation of these cations, which encourage the formation of a two-dimensional structure, increased the bandgap of the materials and improved their thermal stability and humidity. Aunque naturalmente la introducción de estos cationes genera una disminución en las propiedades de transporte, reduciendo la corriente de los dispositivos, se lograron obtener dispositivos con eficiencias de 10,35% para (BUA)2(MA)2Pb3I10, que, presentando una estabilidad mejorada, lograron retener el 68% de fearlessness inicial luego de 1700h sin encapsulamiento.

Introduction

Since the first report by Kojima et al. [1] in 2009, hybrid perovskite materials with the general formula AMX3 (A=Cs+, CH3NH3+, or HC(NH2)2+; M=Pb2+; and X=Cl-, Br-, and I-) have

caught the attention of numerous academics working in the photovoltaic field. The methylammonium (MA) in three dimensions The most promising material for producing high-performance solar cell devices is lead iodide (MAPbI3) [2–5]. The primary benefits of this material are connected with its excellent properties as a satisfactory sun-powered cell safeguard, including little exciton-restricting energy [6], high termination coefficient [7], sufficient band hole [8], and long exciton and charge dispersion lengths [9]. However, the development of lead-based perovskite devices in the future faces two major challenges: the lead's toxicity and the degradation of the material by moisture in the air [10, 11]. The material's improved moisture stability may also aid in reducing lead toxicity because it may prevent

Perovskite that dissolves easily in water Formamidium (FA) has improved thermal stability but not moisture stability when MA has been replaced [12, 13]. However, MA can be substituted for by a wide variety of less water-soluble organic cations. Yet, these bigger cations surpass Goldschmit's resistance factor that decides the arrangement of 3D perovskites [14, 15]. Stable perovskite structures in two dimensions, however, are also simple to obtain. Ruddlesden–Popper layered perovskites with the general formula A2Bn-1PbnI3n+1 are among these 2D stable perovskites. Can transition from simple 2D (n=0) to 3D (n=) The 2D Ruddlesden-Popper (BA)2(MA)n1PbnI3n+1 layered perovskite, in which BA represented the n-butylammonium cation CH3(CH2)3NH3+, was the subject of research by Cao et al. [16]. When n=3, they discovered that the best photovoltaic device had improved moisture stability and an efficiency of 4.02 percent. Afterward, in a similar framework, Tsai et al. [17] Used a hot casting technique to improve the orientation of the films, allowing them to rise from 4.44 percent to 11.44 percent. Phenylethylammonium cation, PhC2H5NH3+ (PEA), was used in a similar 2D Ruddlesden-Popper system in the (PEA)2(MA)2Pb3I10 system. The resulting devices showed improved moisture stability and efficiencies ranging from 4.73 percent to 7.02 percent that were highly dependent on the scan rate (indicating hysteresis) [18]. It is essential to keep in mind that there is still a significant amount of work to be done regarding the layered perovskite structure when options regarding the value of n and the combination of multiple organic cations are taken into consideration [19]. When n=3, the most promising system for 2D Ruddlesden-Popper layered perovskite was found, according to previous research [20]. In order to speed up the development of lead hybrid perovskite solar cells, these findings ought to serve as a starting point for continuing to enhance the stability and performance of these new layered systems. In these systems, the active layer's final properties are determined by the appropriate organic cation selection, as large cations with lower polarity can improve moisture stability while also influencing transport properties across organic chains. Thusly, in this work, we research and report the creation and properties of 3D MAPbI3 and 2D Ruddlesden-Popper layered perovskites with n=3. The three-layered perovskites (PA)2(MA)2Pb3I10, (BUA)2(MA)2Pb3I10, and (BEA)2(MA)2Pb3I10 were created by selecting three organic cations of varying natures, such as n-propylammonium (PA), t-butylammonium (BUA), and benzylammonium (BEA). Due to differences in size, structure, and hydrophobicity; all of the materials had very different photovoltaic properties; however, they all had better moisture stability than the 3D MAPbI3 perovskite. In contrast to PA and The (BUA)2(MA)2Pb3I10 system benefited from enhanced transport properties and adequate moisture tolerance thanks to BEA, the shorter branched BUA cation. Methods of experimentation

Perovskitesynthesis

Organic cations from Dyesol were used, including Methylammonium iodide (MA), Propylammonium iodide (PA), t-Butylammonium iodide (BUA), and Benzylammonium iodide

(BEA). Lead iodide (Alfa Aesar) served as a lead source, and dimethyl sulfoxide (DMSO, Sigma Aldrich) and dimethylformamide (DMF, Alfa Aesar) were utilized as solvents. To get the MAPbI3 antecedent arrangement, Mama and lead iodide were broken down and DMSO (1:1:1 molar proportion; 55% wt.) in N,N-dimethylformamide (DMF, Alfa Aesar) and blended at room temperature for 1h. Similar methods were used to obtain the layered perovskites' precursor solution. The molar ratio was MA: PA, BUA or BEA: lead iodide (2:2:3), and the concentration remained constant. The precursor solutions were spin-coated on top of a glass substrate for 25 seconds at 3500 rpm in an air-filled environment to produce the films. After ten seconds of spinning, 500 mL of Diethyleter (Aldrich) were dropped onto the substrate. The movies were then tempered at 65 oC for 1 min in addition to 100 oC for 10 min.

Devicefabrication

Glass coated with ITO was used to make the devices (Naranjo). The substrates were washed with impartial cleanser (Inmunodet neutro-nonpartisan cleanser) and successively sonicated in DI water, CH3)2CO, and isopropanol. Then, they were treated with bright ozone for 5 min. Spin-coating a NiOx dispersion resulted in the fabrication of the NiOx hole transporting layer. [21] under air conditions for 30 seconds at 3000 rpm and a 3 s ramp. The precursor solution was then spun-coated for 25 minutes at 3500 rpm to deposit all of the perovskite layers. s. 500 mL of Diethyleter (Aldrich) were spun during dropped 10 seconds later onto the substrate. The films were then annealed for one minute at 65 oC and for ten minutes at 100 oC. A 20 mg/mL solution of PCBM (1-Material) was spin-coated in chlorobenzene (CB) at a speed of 2000 rpm for thirty s. A 0.5 mg/L solution of rodhamine 101 was spun coated at 4000 rpm for 30 seconds before being deposited on top of the PCBM layer. Silver electrodes of 100 nm size complete the devices. Were thermally evaporated in a vacuum of 106 mbar at a deposition rate of 0.1 nm s1, producing devicesWith a 0.09 cm2 active area

Characterization

X-ray diffractograms were collected from 2θ=5° to 50° inaBragg-Brentanogeometry, fromthepreparedthinfilmsin a PANalytical diffractometer, utilizing Cu Kθ (1.5408 Å) radiation with a stage size of 0.04° and a speed of 2° each moment. Using a Cary 100 Agilent spectrometer and a Cary Eclipse Agilent spectrometer, optical absorption and photoluminescence were measured in the 400-850 nm range, respectively. The electrical portrayal of the gadgets was performed utilizing a 4200SCS Keithley framework at a voltage cleared speed around 400 mV/s in blend with an Oriel sol3A sun test system, which was adjusted to AM1.5G standard circumstances utilizing an oriel 91150 V reference cell. An Oriel IQE 200 was utilized to decide the outer quantum effectiveness in the scope of 300 to 800 nm. AFM images of the morphology were obtained from Oxford Instruments using a MFP-3D infinity. The samples were connected to an external bias that existed between the ITO substrate and the AFM tip in order to produce photoconductive AFM images using the same equipment. After that, a voltage sweep was done, and the current that was going to the tip was measured. For dark measurements, the samples weren't lit, but for white measurements, they were lit.

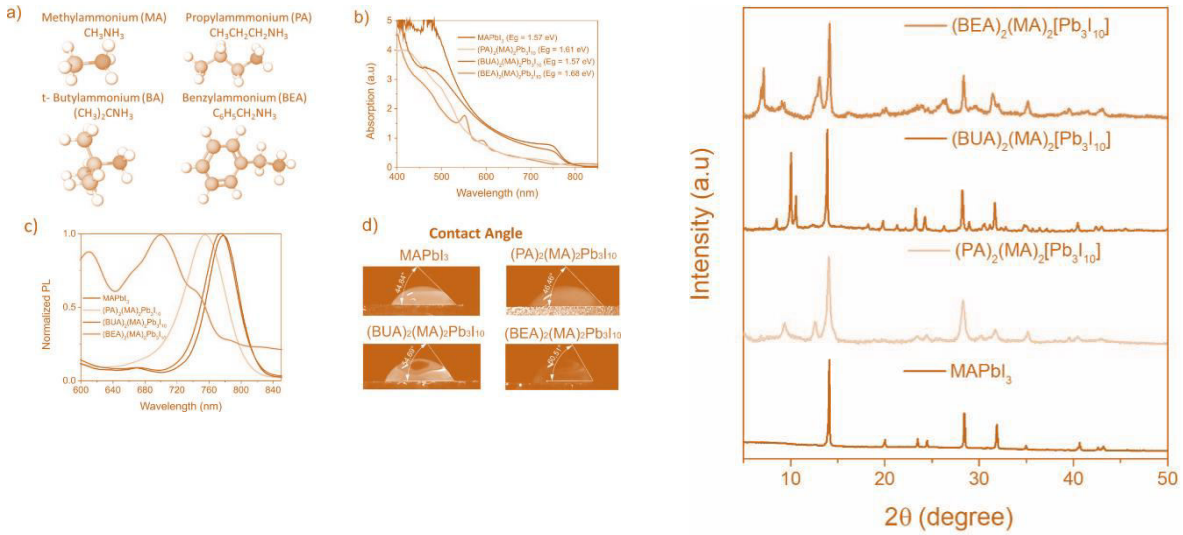

Figure1*Two-layered perovskites. a) Construction of the different natural cations used to combine the layered perovskites. b) Absorption spectra and c) PL intensity for the layered perovskite thin films. d) Photograph of the water drop's contact angle. indicating that the layered perovskites are more hydrophobic.*

Results

Figure 1a depicts the various organic cation structures utilized to produce the hybrid perovskites. Note that n-propylammonium (PA) is a linear compound. Benzylammonium (BEA) is an aromatic cation with one carbon atom and an aromatic phenyl group, while t-butylammonium (BUA) is a branched-chain with four carbon atoms. Because of the expanded substance of carbon molecules according to Methylammonium (Mama), the presentation of these cations makes it conceivable to acquire more hydrophobic designs. However, the tolerance factor [22] indicates that 3D perovskite cannot be produced with large cations. The determined retention beginning expanded with a propensity like size of the natural cation, coming about in 1.57eV for MAPbI3, 1.61eV for (PA)2(MA)2Pb3I10, 1.57eV for (BUA)2(MA)2Pb3I10 and 1.68eV for (BEA)2(MA)2Pb3I10 (Figure 1b) in concordance with the PL emanation as displayed in Figure 1c. The optical band holes (Eg) in the layered materials expanded concerning the 3D perovskite in light of quantum restriction impacts [23]. Similar to other studies on hybrid perovskites, these findings show an increase in the (BA)2(MA)n1PbnI3n+1 series with the decreased inorganic slab thickness from n = to n =1 [16]. Nonetheless, in all cases, the band hole shift is not extremely set apart because of the presence of layer-edge-states (LES), showing that the excitons are nearly ionized into free transporters at room temperature, giving a pathway for separating excitons into longer-lived free-transporters [24]. For photovoltaic applications, the efficient PL found in all samples is crucial because It is a sign of carrier generation, which makes it possible to access the highest open-circuit voltage. [25] Take note of the fact that, in accordance with the exciton absorption in the 500 nm to 550 nm range, the largest BEA cation displayed three distinct emission peaks. On the other hand, we also kept an eye on how the hydrophobicity of the film changed. The droplet's contact angle is shown in Figure 1d as water (7 L) increased in proportion to the organic cation's size. expanded, going from 44.84° for MAPbI3 to 60.51° for (BEA)2(MA)2Pb3I10. The increased resistance to moisture should also be reflected in this improvement in the contact angle. X-ray diffraction (XRD) confirmed the obtained materials' structural integrity. The new peaks at low diffraction angles confirm that hybrid layered

perovskites were created by altering the MAPbI3 perovskite's 3D structure, as depicted in Figure 2. The layered materials related to (PA)2(MA)2Pb3I10, (BUA)2(MA)2Pb3I10, and (BEA)2(MA)2Pb3I10, a result of cutting the 3D perovskite into obvious 2D chunks.

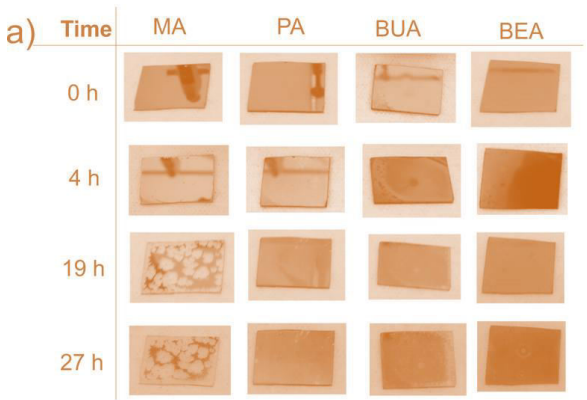

Figure2*ExperimentalXRDspectraforthree-dimensionalperovskite(MAPbI3)andthetwo-dimensionalperovskites*

The films were subjected to a moisture stability test at 80 percent in order to investigate the stability of the layered materials. Relative Mugginess. The progression of the films up to a 27-hour exposition time is depicted in Figure 3a. Degradation was very obvious in the MAPbI3 sample, and after 19 hours, transparent yellowish zones formed, indicating perovskite hydration [26]. However, as depicted in Figure 3b, the layered samples were more stable because they began to exhibit significant color changes after 27 hours. The previous indications that larger cations result in more stable films were followed by the stability trend. Additionally, temperature stability is a crucial aspectfor photovoltaic applications because organic cations like formamidinium (FA) have been shown to improve the perovskite's thermal stability [27, 28]. As a result, the films also underwent a 15-day temperature stability test at 85 °C. Similar to the moisture test, the thermal stability of the layered perovskites was higher than that of the 3D MA-based perovskite. This was probably because the large organic cations in the MA were more difficult to volatilize.

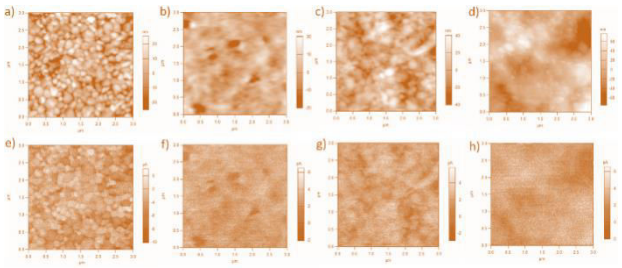

Figure3*2D perovskites' improved resistance to moisture. a) Images of the films and b) Time-dependent absorption decay for the test of moisture stability at an RH of 80%*

As shown in Figure 4a, the morphology of the materials was affected when the large inorganic cations were added to the 2D perovskites. The MAPbI3 sample had a similar morphology, with grains that were well-defined and had an average size of 180 nm. The morphology of the (PA)2(MA)2Pb3I10 perovskite featured less distinct grains embedded in what appeared to be an amorphous phase for the two additional linearly connected carbons. The fact that the layered structure does not have a large-

range 3D continuous order indicates that this phase should correspond to tiny grains that are limited by the PA layer. However, for the situation,

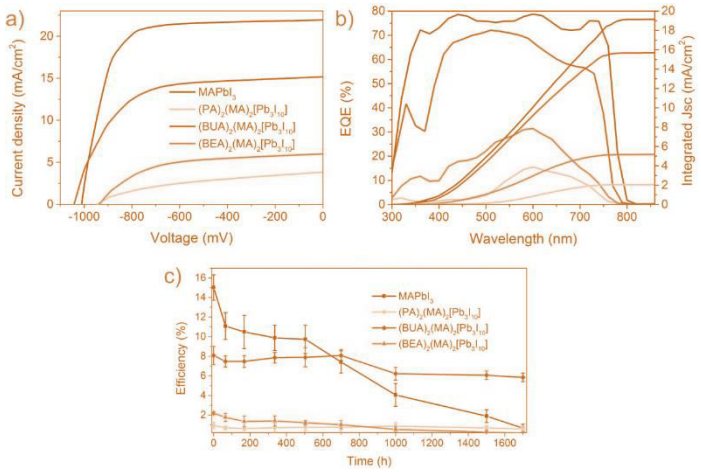

Figure4*a-d) AFM images illustrating the morphology of MAPbI3, (PA)2 (MA)2 Pb3 I10, (BUA)2 (MA)2 Pb3 I10, and for (BEA)2 (MA)2 Pb3 I10 films, respectively. e-h) superposed AFM and photoconductive AFM images illustrating the morphology of MAPbI3, (PA)2 (MA)2 Pb3 I10, (BUA influenced by the continuity of the phase [29] As a result, it would be ideal to have improved resistance to temperature and moisture while its transport properties would be less affected.*

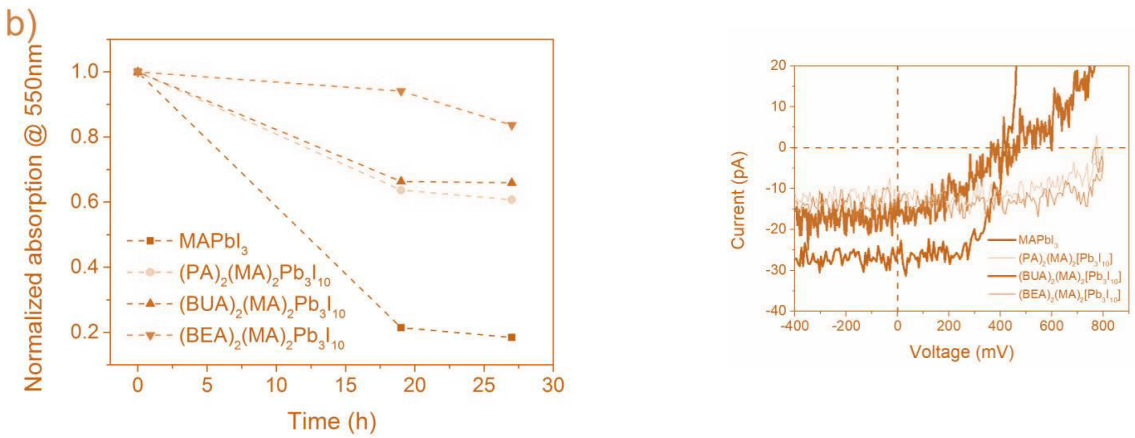

Figure5*J-Vcurveofperovskitefilmsobtainedfromphotoconductive**AFM*

Large grains have been observed in the (BUA)2(MA)2Pb3I10 structure of the BUA cation, which has three additional carbon atoms. This is probably due to the fact that this branched cation only produces a continuous chain of two carbon atoms, making the layer separation shorter than that of the PA cation, as was previously discussed in terms of its smaller unit cell. The phenyl bunch in the BEA cation is the biggest gathering in the layered perovskites; it permitted the development of little grains that are more modest than the ones framed by BUA, yet bigger than those shaped by Dad cations, likely in view of a superior connection between the phenyl gatherings. This distinction in morphology is vital since the vehicle properties of these materials are amazingly to study both, photoactive and transport properties of the movies, photoconductive AFM was performed. While a voltage sweep between -400mV and 800mV was applied, the films were illuminated. As shown in Figure 5, this made it possible to obtain a

J-V curve that was used to compare the photovoltaic properties of the films. Voc increased in the opposite direction due to the larger band gaps of the layered perovskites, but the generated current followed the decreasing order of 3D MAPbI3 >BUA- >BEA-> PA-based 2D perovskites. Figure 4e–4h depicts the superposition of the morphology and photoconductive AFM images. Similar to studies that suggested transport depended on the facets of the material [30], 3D MAPbI3 displayed a clearly defined contrast between the produced current and each grain. The (BUA)2(MA)2Pb3I10 test was the just layered perovskite that delivered some differentiation between grains, showing the nearer conduct to a 3D perovskite. The production of planar photovoltaic devices was facilitated by the uniformity and high quality of the layered perovskite films. Compared to the 3D perovskite, these films produced intriguing results for solar cells. The fabricated devices' photovoltaic performance is summarized in Table 1. The best-performing reference device for the MAPbI3 sample had an average power conversion efficiency of 16.16 percent. The presented devices are (PA)2(MA)2Pb3I10 and (BEA)2(MA)2Pb3I10.

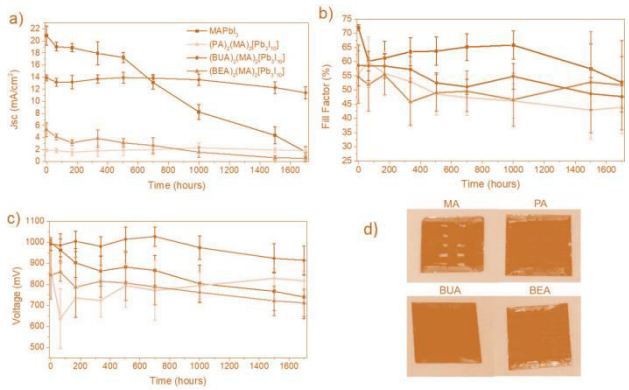

Figure6*Layered perovskites' photovoltaic performance: a representative J-V curve, EQE spectra, and a stability test at 60% Perovskite devices without encapsulation have a R.H of up to 1700 hours.*

A typical effectiveness of 1.10% and 2.19%, separately. The low current that was obtained was primarily responsible for this poor performance. This is to be expected because organic cations, which act as an insulating spacing layer between the inorganic conduction slabs, prevent out-of-plane charge transport in layered systems, resulting in relatively poor efficiency [17]. As a result, one approach to the best results relies on the possibility of having films that have a preferential out-of-plane alignment with respect to the contacts to facilitate efficient charge transport. The (BUA)2(MA)2Pb3I10 layered perovskite material's improved current resulted in improved photovoltaic performance, with a best efficiency of 10.35 percent and an average efficiency of 8.25 percent, respectively. The typical J-V curves for each of the devices that were obtained are depicted in Figure 6a. Figure 6b's EQE confirmed the obtained current, which followed a pattern similar to that of the photoconductive AFM: 3D MAPbI3 >BUA- >BEA-> PA-based 2D perovskites. However, in devices without encapsulation and exposed to 60% R.H., comparative long-term stability measurements for all perovskites were carried out. The effectiveness development for this test is displayed in Figure 6c. The (PA)2(MA)2Pb3I10 and (BEA)2(MA)2Pb3I10 perovskites showed a slower decay, but this improved stability did not provide any advantage due to the low performance. After 1700 h, the efficiency of the 3D perovskite was almost null. In contrast, devices with an average efficiency of 5.98% after 1700 hours were produced by of its initial value. As shown in Figures 7a–7c for Jsc, Voc, and FF decay,

degradation of Jsc was the primary driver of efficiency decline. Figure 7d shows that the MAPbI3 devices began to become transparent, indicating that perovskite hydration [26] was the most likely degradation mechanism for the two-dimensional samples.

Conclusions

We have conducted in-depth research on various hybrid perovskite materials belonging to the Ruddlesden–Popper family. The three large organic cations used to fabricate the layered perovskites showed improved moisture and thermal stability but marked differences in the photovoltaic performance, demonstrating that the proper selection of the organic cations plays an important role in the final perovskite morphology and properties. This was demonstrated by structural characterization and device performance. In addition, devices employing (BUA)2(MA)2Pb3I10 as the active layer achieved an efficiency of 10.35 percent. When exposed to 60%, these unencapsulated devices retained 68% of their performance. R.H throughout the course of 1700 hours, which is superior to the control MAPbI3 devices. PSC stability can be improved by selecting the right organic spacer in a two-dimensional perovskite, as shown by our findings.(BUA)2(MA)2Pb3I10, which retained 68%

References

1. Kojima, K. Teshima, Y. Shirai, and T. Miyasaka, "Organometalhalide perovskites as visible-light sensitizers for photovoltaic cells,"*JournaloftheAmericanChemicalSociety*,vol.131,no.17,Apr.14,2009.[Online].Availab le:https://doi.org/10.1021/ja809598r
2. X.Liand*et al.*, "A vacuum flash–assisted solution processfor high-efficiency large-area perovskite solar cells," *Science*,vol.353,no.6294,Jul.01,2016.[Online].Available:https://doi.org/10.1126/science.aa f8060
3. M. Park, J. S. Park, I. K. Hanb, and J. Y. Oh, "High-performanceflexible and air-stable perovskite solar cells with a large active areabased on poly(3-hexylthiophene) nanofibrils," *Journal of MaterialsChemistry A*, vol. 4,no. 29,Jun. 23,2016. [Online]. Available:https://doi.org/10.1126/science.aaf8060
4. M. M. Lee1, J. Teuscher1, T. Miyasaka, T. N. Murakami, and H. J.Snaith, "Efficient hybrid solar cells based on meso-superstructuredorganometal halide perovskites," *Science*, vol. 338, no. 6107, Nov. 02,2012.[Online].Available:https://doi.org/10.1126/science.1228604
5. W.Chenand*etal.*,"Hybridinterfaciallayerleadstosolidperformanceimprovementofinvertedpe rovskitesolar cells,"*Energy&EnvironmentalScience*, vol.8, no.2,Dec.03, 2014.[OnlineAvailable:https://doi.org/10.1039/C4EE02833C
6. S.Jiangand*etal.*,"Carrierseparationandtransportinperovskitesolarcellsstudiedbynanometre-scaleprofilingofelectrical potential," *Nature Communications*, vol. 6, no. 8397, Sep.28,2015.[Online].Available:https://doi.org/10.1038/ncomms9397
7. H. S. Jung and N. G. Park, "Perovskite solar cells: From materialsto devices," *Small*, vol. 11, no. 1, Jan. 07, 2015. [Online]. Available:https://doi.org/10.1002/smll.201402767
8. T.Baikieand*etal.*,"Synthesisand crystal chemistry of thehybrid perovskite (ch_3nh_3)$pbi_3$for solid-state sensitised solar cellapplications,"*JournalofMaterialsChemistryA*,vol.1,no.18,Mar.12,2013.[Online].Availa ble:https://doi.org/10.1039/C3TA10518K
9. S.D.Stranksand*etal.*,"Electron-holediffusionlengthsexceeding1micrometerinanorganometaltrihalideperovskiteabsorber,"*S cience*,vol. 342,no. 6156,Oct. 18,2013. [Online].

Available:https://doi.org/10.1126/science.1243982
10. S.Guarneraand*etal.*,"Improvingthelong-termstabilityofperovskite solar cells with a porous al2o3 buffer layer," *The JournalofPhysicalChemistryLetters*,vol.6,no.3,Jan.13,2015.[Online].Available:https://doi.org/10.1021/jz502703p
11. K. Wang, Z. Liang, X. Wang, and X. Cui, "Lead replacementinch3 nh3 pbi3perovskites,"*Advanced Electronic Materials*,vol.1,no. 10, Aug. 22, 2015. [Online]. Available:https://doi.org/10.1002/aelm.201500089
12. G. E. Eperon and *et al.*, "Formamidinium lead trihalide:a broadlytunable perovskite for efficient planar heterojunction solar cells,"*Energy&EnvironmentalScience*,vol.7,no.3,Jan.06,2014.[Online].Available:https://doi.org/10.1039/C3EE43822H
13. G. Gordillo, O. Virgüez, C. Otálora, C. Calderón, and C. Quiñones,"Synthesisandoptimizationofpropertiesofthinfilmsoffax(ma1-X)pbi3grown by spin coating with perovskite structuretobeusedasactivelayerinhybridsolarcells,"*RevistaUISIngenierías*,vol.19,no.1,Nov. 27,2010.[Online].Available:https://doi.org/10.18273/revuin.v19n1-2020008
14. V.M.Goldschmidt,"Diegesetzederkrystallochemie,"*Naturwissenschaften*,vol.14,May.1926. [Online].Available:https://doi.org/10.1007/BF01507527
15. T.J.Jacobsson,M.Pazoki,A.Hagfeldt,andT.Edvinsson,"Goldschmidt´s rules and strontium replacement in lead halogenperovskitesolarcells: Theory and preliminary experiments onch3 nh3 sri3 ," *The Journal of Physical Chemistry C*, vol. 119, no. 46,Oct. 26, 2015. [Online]. Available: https://doi.org/10.1021/acs.jpcc.5b06436
16. H. Cao, C. C. Stoumpos, O. K. Farha, J. T. Hupp, andM. G.Kanatzidis,"2d homologous perovskites aslight-absorbingmaterialsforsolarcellapplications,"*JournaloftheAmericanChemical Society*, vol. 137, no. 24, May. 28, 2015. [Online]. Available:https://doi.org/10.1021/jacs.5b03796
17. H.Tsaiand*etal.*,"High-efficiencytwo-dimensionalruddlesden–popper perovskite solar cells," *Nature*, vol. 536, Jul. 06,2016.[Online].Available:https://doi.org/10.1038/nature18306
18. C.Smith,E.T.Hoke,D.Solis,M.D.McGehee,andH.I.Karunadasa, "A layered hybrid perovskite solar cell absorber withenhancedmoisturestability,"*Angewandte*,vol.126,no.42,Oct.13,2014.[Online].Available:https://doi.org/10.1002/ange.201406466
19. Ramírez and *et al.*, "Layered mixed tin–lead hybrid perovskitesolarcellswithhighstability,"*ACSEnergyLetters*,vol.3,no.9,Aug.25, 2018. [Online]. Available: https://doi.org/10.1021/acsenergylett.8b01411
20. Y. Dong, D. Lu, Z. Xu, H. Lai, andY.Liu,"2-thiopheneformamidinium-based2druddlesden-popperperovskitesolarcellswithefficiencyof16.72%andnegligiblehysteresis," *Advanced Energy Materials*, vol. 10, no. 28, Jun. 05, 2020.[Online].Available:https://doi.org/10.1002/aenm.202000694
21. J.Ciroand*etal.*,"Self-functionalizationbehindasolution-processednioxfilmusedasholetransportinglayerfor efficient perovskitesolarcells,"*ACSAppliedMaterials&Interfaces*,vol.9,no.14,Mar.28,2017.[Online].Available:https://doi.org/10.1021/acsami.6b15975
22. G.Kieslich,S.Sun, and A. K. Cheetham, "An extendedtolerancefactorapproachfororganic–inorganicperovskites,"*ChemicalScience*,vol.6,Apr.14,2015.[Online].Available:https://doi.o

rg/10.1039/C5SC00961H

23. R.L.Milotand*etal.*,"Charge-carrierdynamicsin2dhybridmetal–halideperovskites,"*Nano Letters*, vol. 16, no. 11, Sep.30, 2016. [Online]. Available:https://doi.org/10.1021/acs.nanolett.6b03114
24. J.C.Blanconand*etal.*,"Extremelyefficientinternalexcitondissociationthroughedgestatesinlayered2dperovskites,"*Science*,vol. 355,no. 6331,Mar. 24,2017. [Online]. Available:https://doi.org/10.1126/science.aal4211
25. O. D. Miller, E. Yablonovitch, and S. R. Kurtz, "Stronginternal and external luminescence as solar cells approachthe shockley-queisser limit," *IEEE Journal of Photovoltaics*,vol.2,no.3,Jun.06,2012.[Online].Available:https://doi.org/10.1109/JPHOTOV.2012.2198434
26. M.A.Leguy,"Reversible hydrationof ch3 nh3 pbi3in films,single crystals, and solar cells," *Chemistry and Materials*, vol. 27,no.9,Apr.05,2015.[Online].Available:https://doi.org/10.1021/acs.chemmater.5b00660
27. J. W. Lee, D. J. Seol, A. N. Cho, and N. G. Park, "High-efficiencyperovskite solar cells based on the black polymorph ofhc(nh2)2 pbi3 ," *Advanced Materials*, vol. 26, no. 29, Aug. 06, 2014.[Online].Available:https://doi.org/10.1002/adma.201401137
28. J.W.Leeand*etal.*,"Formamidiniumandcesiumhybridizationforphotoandmoisturestableperovskitesolarcell,"*AdvancedEnergy Materials*, vol. 5, no. 20, Oct. 21, 2015. [Online]. Available:https://doi.org/10.1002/aenm.201501310
29. S.ChenandG.Shi,"Twodimensionalmaterialsforhalideperovskitebased optoelectronic devices," *Advanced Materials*, vol. 29, no. 24,Mar. 03,2017. [Online]. Available:https://doi.org/10.1002/adma.201605448
30. G. E. Eperon and D. S. Ginger, "Perovskite solar cells:Differentfacets of performance," *Nature Energy*, vol. 1, no. 16109, Jul. 04,2016.[Online].Available:https://doi.org/10.1038/nenergy.2016